

Supplementary Information

Gold nanocrystals anchored In₂O₃ hollow nanospheres for N₂ photofixation to ammonia

Ri Han^{a,b}, Shufang Chang^a and Xiaoxiang Xu^{*a,b}

*^aShanghai Key Lab of Chemical Assessment and Sustainability, School of Chemical
Science and Engineering, Tongji University, 1239 Siping Road, Shanghai, 200092,
China. E-mail: xxxu@tongji.edu.cn; Tel: +86-21-65986919*

*^bClinical and Central Lab, Putuo People's Hospital, Tongji University, 1291
Jiangning Road, Shanghai, 200060, China*

List of Content

Page S4-S8 Method for materials synthesis and characterization

Page S9 Figure S1. X-ray powder diffraction (XRD) patterns of as-prepared In₂O₃ HS, Au@ In₂O₃ HS, Au loading is fixed at 1 wt%. Commercial In₂O₃ (99.99%, Aladdin, China) was also included and was designated as In₂O₃ Bulk. In₂O₃ Bulk was also loaded with the same amounts of Au and was designated as Au@In₂O₃ Bulk. Standard patterns for In₂O₃ (JCPDS: 00-006-0416) was also added for comparisons.
(b) Rietveld refinement of XRD patterns for In₂O₃ HS, the refinement converges with good *R* and χ^2 parameters ($R_p = 4.38\%$, $R_{wp} = 4.50\%$, $\chi^2 = 1.058$).

Page S10 Figure S2. EDX-mapping analysis of Au@In₂O₃ HS

Page S10 Figure S3. SEM image of Au@In₂O₃ Bulk: (a) low resolution and (b) high resolution.

Page S11 Figure S4. Normalized ammonia production rate of Au@In₂O₃ HS and Au@In₂O₃ Bulk

Page S11 Figure S5. Calibration for ammonia determination using indophenol-blue method: (a) Absorption spectra for the testing solution containing NH₄⁺ at different concentrations; (b) linear relationship between the absorption at 697 nm and NH₄⁺ concentration.

Page S12 Figure S6. (a) Calibration curve for ammonia determination using ion chromatography method; (b) representative ion chromatographs of Au@In₂O₃ HS aliquots during nitrogen-fixation after illumination for 2 h, NH₄⁺ has a retention time around 10.6 min; (c) ammonia production rate of Au@In₂O₃ HS determined using ion chromatography method; data obtained by indophenol-blue method were also shown for comparisons.

Page S12 Figure S7. Photocatalytic NH₃/ND₃ production rate of Au@In₂O₃ HS using H₂O and D₂O as the proton source

Page S13 Figure S8. Temporal photocatalytic oxygen evolution of Au@In₂O₃ HS, the reactor was sealed after purging the reactor with N₂. Sampling of the gas in the reactor was performed by using a syringe every 30 min and the gas was analyzed by a gas chromatograph (TECHCOMP, GC7900) equipped with a thermal conductivity detector and 5 Å molecular sieve columns. Ar is used as the carrier gas.

Page S14 Figure S9. (a) XRD patterns of Au@ In₂O₃ HS before and after photocatalytic experiment; SEM image of Au@ In₂O₃ HS before (b) and after (c) photocatalytic experiment

Page S14 Figure S10. XPS spectra of O 1s state for Au@ In₂O₃ HS in variance with different Au amounts.

Page S15 Figure S11. The electron paramagnet resonance (EPR) spectra of Au@ In₂O₃ HS

Page S15 Figure S12. (a) Mott-Schottky (MS) analysis of In₂O₃ HS; (b) XPS valence band scan of In₂O₃ HS and (c) band edge positions of In₂O₃ HS. Band edge positions were deduced by combining MS analysis and XPS valence band scan: the extrapolating the linear part of MS curve gives flat band potential of In₂O₃ HS (-0.56 eV vs NHE). XPS valence band scan informs the energy difference between valence band edge and Fermi level (i.e. flat band potential) which is 1.85 eV. The valence band edge position can be deduced to be 1.29 V vs NHE. Considering the band gap of In₂O₃ HS (i.e. 2.8 eV), the conduction band edge can be determined.

Page S16 Table S1. BET surface area of as-prepared sample powders.

Page S16 References

Materials synthesis

Hollow In_2O_3 nanospheres were fabricated using carbon nanospheres as templates. The carbon nanospheres were synthesized by hydrothermal method according to previous reports^{1, 2}. Specifically, 20 mL glucose (98%, Aladdin) aqueous solution (1 M) was transferred into Teflon-lined stainless-steel autoclave (100 mL). The reactor was heated to 250 °C at a heating rate of 1 °C/min, maintained at 250 °C for 12 h and then cooled naturally. The product was black suspensions which were centrifuged to separate the solid. The solid was rinsed by deionized water five times and was dried in an oven at 80 °C. SEM analysis suggests they are carbon nanospheres with a diameter of ca. 200-500 nm. These freshly prepared carbon nanospheres were used as the templates for subsequent synthesis without further treatment.

In a typical synthesis of hollow In_2O_3 nanospheres, 0.5 g carbon nanospheres were dispersed into 50 mL InCl_3 (99.9%, Aladdin) aqueous solution (20 mM) under magnetic stirring. The suspensions were then transferred into a Teflon-lined stainless-steel autoclave (100 mL) and were heated at 180 °C for 6 h. The precipitants obtained were separated by centrifugation, rinsed by deionized water and ethanol (99.5%, SCR), dried at 60 °C and calcined at 500 °C for 5 h in air. The resultant yellow powders were designated as In_2O_3 HS. Commercial In_2O_3 powders (99.99%, Aladdin, China) were used for comparison purpose and were designated as In_2O_3 Bulk.

Anchoring Au nanocrystals onto In_2O_3 HS was performed by photoreduction method.

Typically, 50 mg In_2O_3 HS was dispersed into 5 mL HAuCl_4 (99.5%, SCR) aqueous solution (1 mg/mL) under sonication. The suspensions were illuminated under 365 nm UV light for 5 min. The color of the suspensions changed rapidly, indicating successful anchorage of Au nanocrystals. The precipitants were centrifuged, rinsed by deionized water and ethanol, dried in vacuum at 60 °C for 12 h. The amounts of Au anchored were controlled by varying the concentration of HAuCl_4 aqueous solution in the initial step. Commercial In_2O_3 (99.99%, Aladdin, China) was also anchored with Au nanocrystals using the same procedures and was designated as Au@ In_2O_3 Bulk.

Materials characterization

The phase purity and crystal structure of sample powders were inspected by X-ray powder diffraction (XRD) techniques on a Bruker D8 Focus diffractometer. The incident X-ray radiation was Cu $K_{\alpha 1}$ ($\lambda = 1.5406\text{\AA}$) and Cu $K_{\alpha 2}$ ($\lambda = 1.5444\text{\AA}$). A typical step size was 0.01° and during for data collection time was 0.1 s at each step. General Structure Analysis System (GSAS) software package was applied to perform Rietveld refinement on XRD data collected. Microstructures of freshly prepared samples were examined using a field emission scanning electron microscopy (Hitachi S4800) equipped with a Mica energy dispersive X-ray spectroscopy (EDX) analysis system and also investigated on a transmission electron microscope (JEOL JEM-2100). Surface state of as-prepared samples was analyzed using X-ray photoelectron spectroscopy (Thermo Escalab 250 with a monochromatic Al $K\alpha$ source). All binding energies were referred to adventitious carbon C 1s peak at 284.7 eV. The XPS

PEAKFIT software was also used to fit and analyze the XPS data. Diffuse reflectance spectra were collected on an UV–Vis spectrophotometer coupled with integrating sphere (JASCO-750). BaSO₄ was used as reference non-absorbing material.

N₂ photofixation

The N₂ photofixation reaction was performed in a top-irradiation-type quartz reactor. Sample powders (50 mg) and water (90 mL) were added into the reactor under vigorous stirring. The suspensions were then sonicated for 30 min, followed by bubbling high-purity N₂ gas (80 mL·min⁻¹) for 1 h to remove air dissolved in the suspensions. A Hg lamp (Merc-500 W) was adopted as the light source. An aliquot of suspensions (5.0 mL) was taken out and filtered using a 0.22μm filter to remove sample powders before sampling. The concentration of ammonia in the supernatant was determined using the indophenol-blue method on a UV-Vis spectrophotometer following previous report³. A calibration curve was first determined (see Figure S5) and was used to calculate the amounts of ammonia produced. For each sample, N₂ photofixation experiments were repeated three times and average data with standard deviation was used for comparisons and analysis. Other product of nitrogen photofixation such as N₂H₄ was also detected by a colorimetry method with p-dimethylaminobenzaldehyde (AR, Macklin)⁴. No N₂H₄ signal was detected for a 5 h illumination period. Isotopic labelled experiments were performed by replacing H₂O with D₂O (99%, Aladdin, China) for nitrogen photofixation and other experiment conditions were kept the same. The production of ammonia was also verified by ion

chromatography method. This was performed on Shimadzu IC-2010plus with a cation exchange column equipped with an electrolytically regenerated suppressor. 20 mM methanesulfonic acid was used as the eluent with a flow rate of 1 mL/min. NH_4^+ has a retention time (Rt) around 10.6 min. The amount of ammonium obtained could be estimated very accurately with a calibration curve (Figure S6a), obtained from concentrations in the range from 2 μM to 2 mM. Aliquots collected were diluted ten times for ion chromatography measurements. Calibration curves were calculated by plotting area of the curve (in $\mu\text{S} \times \text{minutes}$, obtained via Chromeleon software package, Thermofischer Scientific Corporation) vs. concentration of the standard (Figure S6a). Final concentration of the aliquots was estimated from the area of the curve for the respective cation (Figure S6b).

Photoelectrochemical (PEC) measurements

Photoelectrode deposited with sample powders were used for PEC measurement. This was done by electrophoretic deposition method⁵: two pieces of fluorine-doped tin oxide (FTO) glass were cut into the proper size (30 \times 10 mm) for deposition. The glasses were rinsed several times with anhydrous alcohol and deionized water under ultrasonic conditions. A 50 mg amount of sample powders and 10 mg of iodine were dispersed into 20 mL of acetone ultrasonically to form suspensions. The FTO glasses were inserted in parallel into the suspensions with conductive sides facing inward. A potentiostatic control (Keithley 2450 Source Meter) was as the use to apply constant

bias (15 V) between the two FTO glasses. Typical deposition time was 3 min. The FTO deposited with sample powders was heated at 673 K for 1 h to remove iodine as was used as the photoelectrode. To improve the connectivity of sample particles and reduce the level of naked FTO, a post-treatment on these electrodes was performed: a few drops of diluted TiCl_4 (Alfa Aesar, 99.9%) methanol solution (10 mM) was dropped onto the photoelectrode and was dried at 623 K for 15 min. This treatment was repeated for five times before the photoelectrodes were calcined at 673 K for 30 min. A three-electrode setup using a Zahner electrochemical workstation was configured for PEC measurements. The as-prepared photoelectrode, Pt foil (10×10 mm) and Ag/AgCl were used as the working, counter, and reference electrodes respectively. $\text{K}_3\text{PO}_4/\text{K}_2\text{HPO}_4$ (0.1 M) aqueous solution (pH = 12.66) was used as the electrolyte and a buffer. A 300 W Xenon lamp (Perfect Light, PLX-SXE300) was used as the light source. The light beam was controlled by an electronic timer and shutter (DAHENG, GCI-73) to rectify the incident light. For Mott-Schottky (MS) analysis, impedance measurements were performed in dark. An AC signal of 1000 Hz and 10 mV amplitude was applied and capacitance was extracted from the impedance data and was used for MS plot.

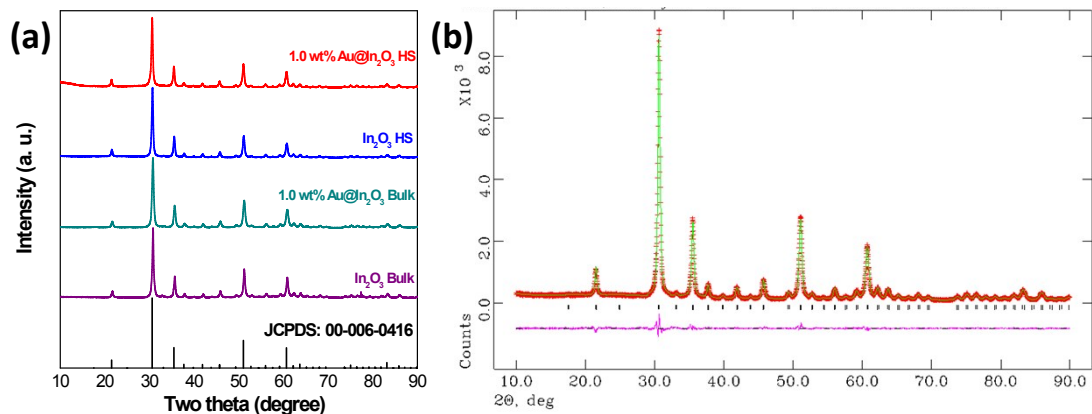


Figure S1. X-ray powder diffraction (XRD) patterns of as-prepared In_2O_3 HS, $\text{Au}@$ In_2O_3 HS, Au loading is fixed at 1 wt%. Commercial In_2O_3 (99.99%, Aladdin, China) was also included and was designated as In_2O_3 Bulk. In_2O_3 Bulk was also loaded with the same amounts of Au and was designated as $\text{Au}@$ In_2O_3 Bulk. Standard patterns for In_2O_3 (JCPDS: 00-006-0416) was also added for comparisons. (b) Rietveld refinement of XRD patterns for In_2O_3 HS, the refinement converges with good R and χ^2 parameters ($R_p = 4.38\%$, $R_{wp} = 4.50\%$, $\chi^2 = 1.058$).

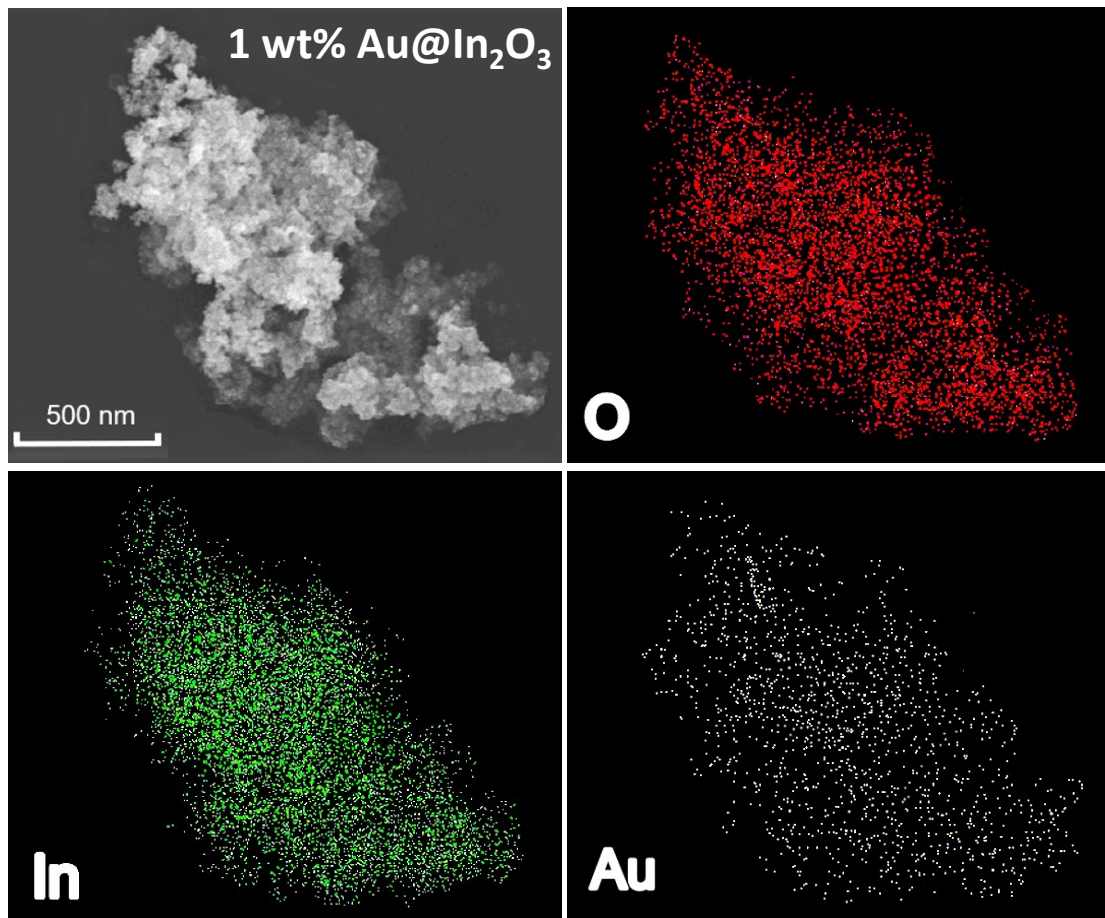


Figure S2. EDX-mapping analysis of Au@ In₂O₃ HS

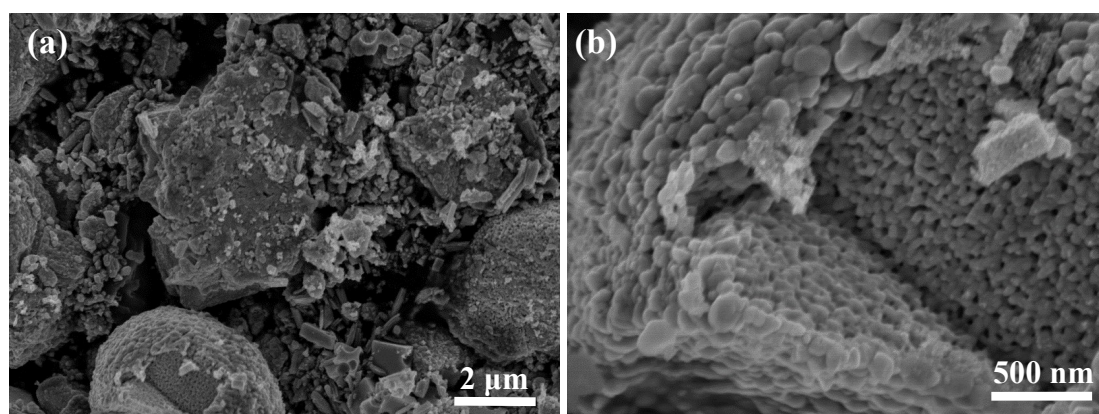


Figure S3. SEM image of Au@ In₂O₃ Bulk: (a) low resolution and (b) high resolution.

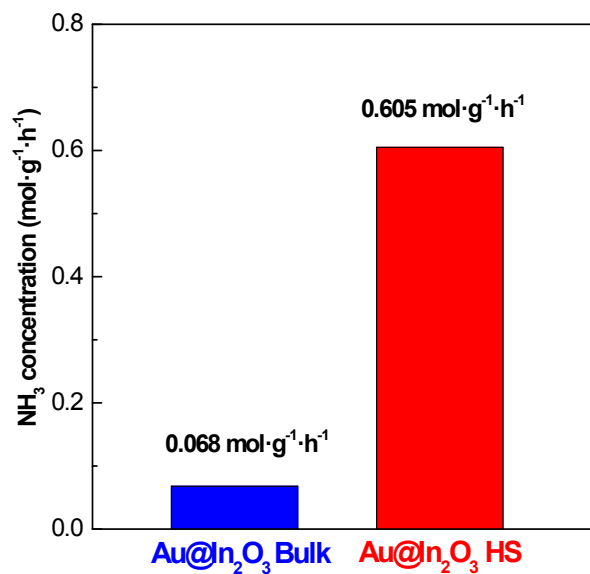


Figure S4. Normalized ammonia production rate of Au@In₂O₃ HS and Au@In₂O₃ Bulk

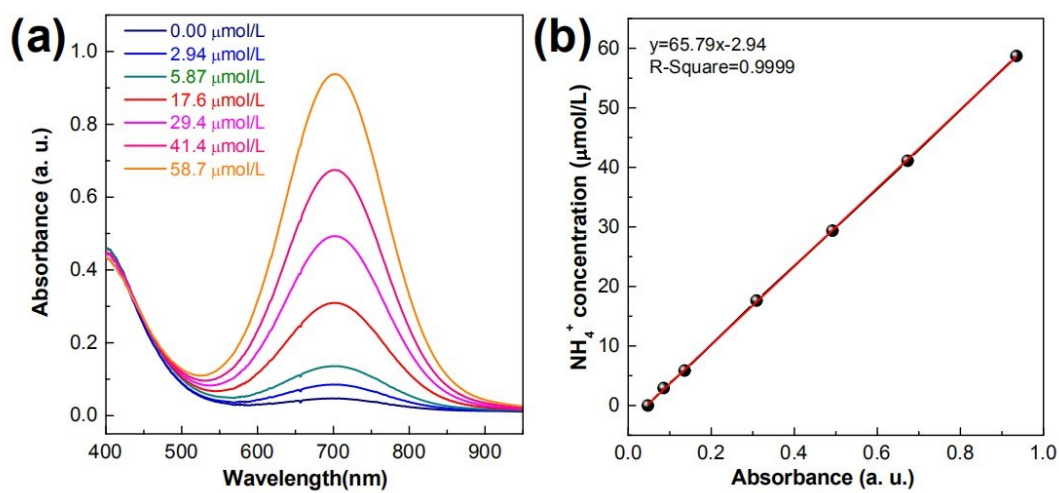


Figure S5. Calibration for ammonia determination using indophenol-blue method: (a) Absorption spectra for the testing solution containing NH₄⁺ at different concentrations; (b) linear relationship between the absorption at 697 nm and NH₄⁺ concentration.

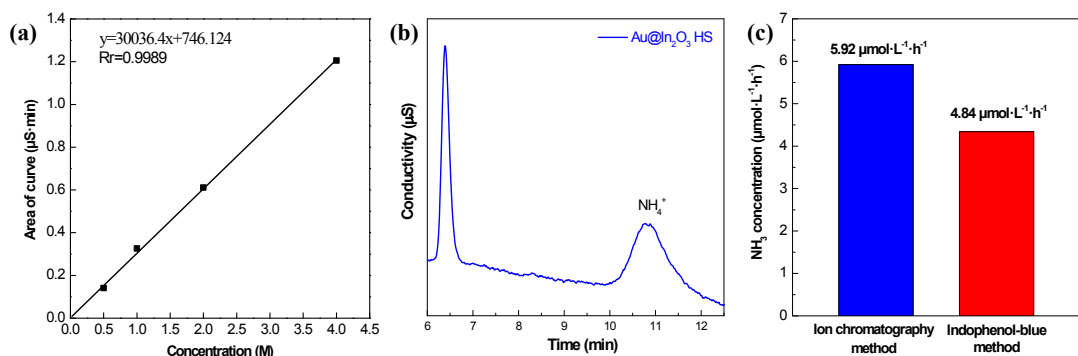


Figure S6. (a) Calibration curve for ammonia determination using ion chromatography method; (b) representative ion chromatographs of Au@In₂O₃ HS aliquots during nitrogen-fixation after illumination for 2 h, NH₄⁺ has a retention time around 10.6 min; (c) ammonia production rate of Au@In₂O₃ HS determined using ion chromatography method; data obtained by indophenol-blue method were also shown for comparisons.

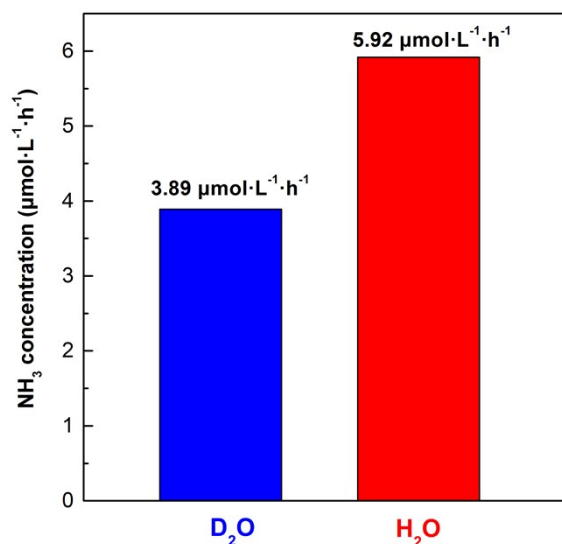


Figure S7. Photocatalytic NH₃/ND₃ production rate of Au@In₂O₃ HS using H₂O and D₂O as the proton source

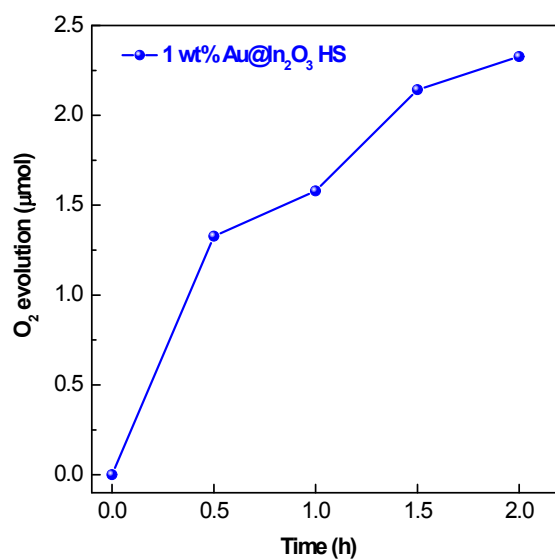


Figure S8. Temporal photocatalytic oxygen evolution of Au@In₂O₃ HS, the reactor was sealed after purging the reactor with N₂. Sampling of the gas in the reactor was performed by using a syringe every 30 min and the gas was analyzed by a gas chromatograph (TECHCOMP, GC7900) equipped with a thermal conductivity detector and 5 Å molecular sieve columns. Ar is used as the carrier gas.

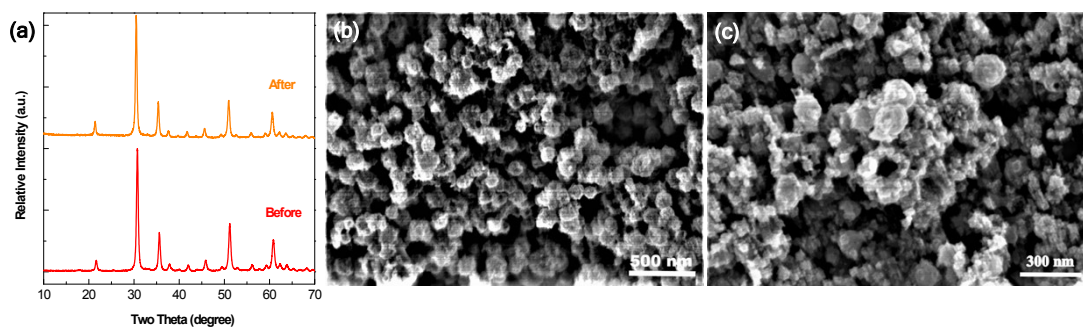


Figure S9. (a) XRD patterns of Au@ In₂O₃ HS before and after photocatalytic experiment; SEM image of Au@ In₂O₃ HS before (b) and after (c) photocatalytic experiment

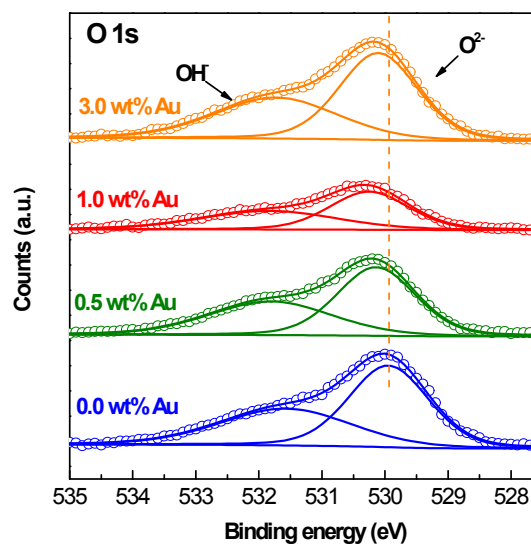


Figure S10. XPS spectra of O 1s state for Au@ In₂O₃ HS in variance with different Au amounts.

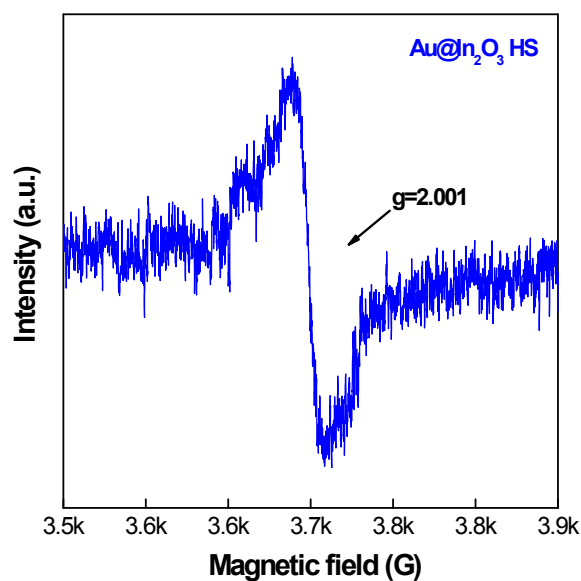


Figure S11. The electron paramagnet resonance (EPR) spectra of Au@ In_2O_3 HS

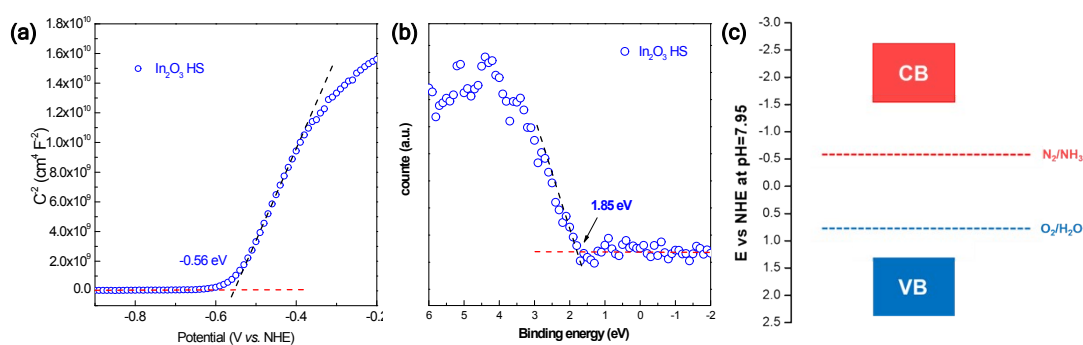


Figure S12. (a) Mott-Schottky (MS) analysis of In_2O_3 HS; (b) XPS valence band scan of In_2O_3 HS and (c) band edge positions of In_2O_3 HS. Band edge positions were deduced by combining MS analysis and XPS valence band scan: the extrapolating the linear part of MS curve gives flat band potential of In_2O_3 HS (-0.56 eV vs NHE). XPS valence band scan informs the energy difference between valence band edge and Fermi level (i.e. flat band potential) which is 1.85 eV. The valence band edge position can be deduced to be 1.29 V vs NHE. Considering the band gap of In_2O_3 HS (i.e. 2.8 eV), the conduction band edge can be determined.

Table S1. BET surface area of as-prepared sample powders.

Sample	BET surface area (m ² ·g ⁻¹)
In ₂ O ₃ Bulk	18.3
In ₂ O ₃ HS	20.0
0.5 wt% Au@ In ₂ O ₃ HS	20.3
1.0 wt% Au@ In ₂ O ₃ HS	20.6
3.0 wt% Au@ In ₂ O ₃ HS	20.6

References

1. M. Sevilla and A. B. Fuertes, The production of carbon materials by hydrothermal carbonization of cellulose, *Carbon*, 2009, **47**, 2281-2289. **DOI:** 10.1016/j.carbon.2009.04.026
2. M. Sevilla and A. B. Fuertes, Chemical and Structural Properties of Carbonaceous Products Obtained by Hydrothermal Carbonization of Saccharides, *Chem-Eur. J.*, 2009, **15**, 4195-4203. **DOI:** 10.1002/chem.200802097
3. S. F. Chang and X. X. Xu, Au nanocrystals decorated TiO₂ nanotubes for photocatalytic nitrogen fixation into ammonia, *Inorg. Chem. Front.*, 2020, **7**, 620-624. **DOI:** 10.1039/c9qi01287g
4. G. N. Schrauzer and T. D. Guth, Photolysis of Water and Photoreduction of Nitrogen on Titanium-Dioxide, *J. Am. Chem. Soc.*, 1977, **99**, 7189-7193. **DOI:** 10.1021/ja00464a015
5. Y. W. Wang, D. Z. Zhu and X. X. Xu, Zr-Doped Mesoporous Ta₃N₅ Microspheres for Efficient photocatalytic water oxidation, *ACS Appl. Mater. Inter.*, 2016, **8**, 35407-35418. **DOI:** 10.1021/acsami.6b14230